

RESEARCH

Open Access



Modified rank sum nonparametric CFAR to combat clutter edge

Meng Xiangwei^{1*}  and Meng Yuan²

*Correspondence:
mengxw163@sohu.com

¹ Department of Electrical and Electronic Engineering, Yantai Nanshan University, Yantai, China

² Department of Computing, The Hong Kong Polytechnic University, Hung Hom, Hong Kong, China

Abstract

The classical rank sum (RS) nonparametric constant false alarm rate (CFAR) detector plays an important role in the theoretical study and practical application of radar target detection. In order to improve the ability of the classical RS nonparametric detector to control the false alarm rate at clutter edges, a modified rank sum (MRS) nonparametric CFAR based on the mean ratio of the samples in the leading and lagging windows is proposed. The analytical expressions of the detection probability and false alarm rate of the MRS nonparametric CFAR in homogeneous background and at clutter edges are derived, and a comparison to the performance of the classical RS nonparametric detector along with some conventional parametric CFAR schemes in homogeneous background, multiple targets situation and clutter edges is made. The numerical results show that the detection performance of the MRS nonparametric CFAR in homogeneous background and in a moderate number of interfering targets situation is close to that of the classical RS nonparametric detector, and its ability to control the rise of the false alarm rate at clutter edges is evidently improved.

Keywords: Radar detection, CFAR, Nonparametric detection, Nonhomogeneous background

1 Introduction

The constant false alarm rate (CFAR) detector is one of the most important parts of modern radar signal processing. It can be used to avoid computer overloading, which is caused by unknown and time-varying clutter background, and obtain high detection performance. Although the CFAR technique has been researched for several decades, the requirement from diverse engineering applications still drives it to continuously develop and progress [1–5]. The simplest one of the CFAR detectors is the cell-averaging (CA) scheme which estimates the noise level in the test cell by averaging the outputs of nearby resolution cells. Although the CA-CFAR gives a minimum loss of detection power in a homogeneous background, it exhibits an intolerable rise in false alarm probability at clutter edges and significant degradation in detection probability in multiple targets situation. In order to alleviate the problems associated with clutter power transitions and the presence of strong returns among the reference samples, the greatest-of (GO) CFAR and the smallest-of (SO) CFAR have been introduced. The GO-CFAR does a better job of maintaining CFAR at clutter edges at the expense of poor resolution of closely spaced targets. The SO-CFAR performs

very well in resolving two closely spaced targets, but experiences even more false alarms than the CA-CFAR in the clutter edge environment. The ordered-statistic (OS) CFAR selects the k th largest sample in the reference window to set an adaptive threshold, thus it has a special immunity to extraneous targets. However, it fails to prevent an excessive false alarm rate at clutter edges unless the threshold estimate incorporates the ordered sample near the maximum. In order to take advantage of the CA-CFAR, the GO-CFAR and the SO-CFAR, an excellent composite approach called as variability index (VI) CFAR was proposed by Smith and Varshney [6]. The VI-CFAR exhibits low loss CFAR performance in a homogeneous environment, has a good false alarm regulation property at clutter edges, and perform robustly when interfering targets are only located at one side of the cell under test.

The CFAR algorithms can be divided into two categories depending upon whether or not a known distribution form is assumed for noise/clutter background: the parametric CFAR and the nonparametric or distribution-free detection methods. The aforementioned CFAR schemes belong to the parametric CFAR type. The parametric CFAR detector suffers from the disadvantage that the detection threshold is sensitive to changes in the background noise/clutter distribution. Even if the distribution of the noise data is known at some time, uncontrollable phenomena may cause changes such that at a later time the clutter distribution is vastly different. These changes will make the performance of the parametric CFAR procedure based on the “known” distribution degrade, whereas the nonparametric CFAR procedures will exhibit its advantage that it can maintain a constant false alarm rate in spite of changes in the underlying data distribution. The most commonly used nonparametric CFAR detection procedures are the classical rank sum (RS) detector and rank quantization (RQ) detector [7]. The RS nonparametric detector was first proposed by Hansen and Olsen [8], and it was called as the generalized sign test detector, and it also was presented in [9] at the same time where it was termed as detector B. The closed-form of P_{fa} of the RS nonparametric detector in homogeneous background has been derived by Akimov (in Russian) and was also reported by Sekine and Mao [10]. The analytical expression of P_{fa} for the RS nonparametric detector at clutter edge was derived in [11], and a comparison of the performance of the RS nonparametric detector in nonhomogeneous background to that of the CA-CFAR, the GO-CFAR and the OS-CFAR with noncoherent integration was made. It is shown that the ability of the RS detector to control the rise of the false alarm rate at clutter edge is even poorer than that of the OS-CFAR with incoherent integration in a Gaussian background.

In order to improve the ability of the classical RS nonparametric CFAR to control the false alarm rate at clutter edges, a modified RS nonparametric (MRS) CFAR is proposed in this work based on the mean ratio of the samples in the leading and lagging windows. The detection principle of the MRS nonparametric CFAR is described in Sect. 2, and its mathematical models for the detection probability and false alarm rate are given in Sect. 3. The numerical and analytical results are given in Sect. 4. Finally, we summarize and discuss the results obtained in this work.

2 The detection principle of the MRS nonparametric CFAR

The block diagram of the MRS nonparametric CFAR detector is shown in Fig. 1. It is assumed that a radar transmits several pulses per antenna beamwidth (or per beam position, in the case of an electronically steerable antenna). For each of M successive

pulses, the radar video output is sampled in range by the range resolution cells, and the resulting samples are stored in a shift register of length $N + 1$. The $N + 1$ samples correspond to a test cell centered in N reference cells. To prevent the target signal energy from spilling over into the adjacent range cells, the guard cells (which are depicted in shadow) directly adjacent to the test cell are used. On the i th pulse ($i = 1, 2, \dots, M$), the sample in the cell under test is denoted as v_i , the sample in the leading window is represented by x_{ij} ($i = 1, 2, \dots, M, j = 1, 2, \dots, N/2$), and that in the lagging window by y_{ij} ($i = 1, 2, \dots, M, j = 1, 2, \dots, N/2$). Here, all of samples x_{ij} in the leading window form the set X , and all of samples y_{ij} in the lagging window form the set Y . In order to improve the ability of the classical RS nonparametric CFAR to control the false alarm rate at clutter edges, the MRS nonparametric CFAR will select the appropriate sample set for the noise/clutter power estimation. That is, the MRS nonparametric CFAR will choose either of the whole samples in the reference window $X \cup Y$, the samples in the leading window X or the samples in the lagging window Y for the adaptive target detection. In principle, the MRS nonparametric CFAR consists of two main steps in implementation, which is described below in detail.

Step 1 Calculation of the mean ratio (MR) statistic.

The MR [6] is defined as the ratio of the mean value of the leading reference window cells and that of the lagging reference window cells as given by (1)

$$MR = \frac{M_X}{M_Y} = \frac{\sum_{i=1}^M \sum_{j=1}^{N/2} x_{ij}}{\sum_{i=1}^M \sum_{j=1}^{N/2} y_{ij}} \tag{1}$$

where M_X and M_Y is the leading and lagging reference window mean, respectively. That is, $M_X = \frac{2}{MN} \sum_{i=1}^M \sum_{j=1}^{N/2} x_{ij}$ and $M_Y = \frac{2}{MN} \sum_{i=1}^M \sum_{j=1}^{N/2} y_{ij}$.

The MR is compared with a threshold K_{MR} and its reciprocal K_{MR}^{-1} to decide if the population means in the leading and lagging window are the same or different using the following hypothesis test:

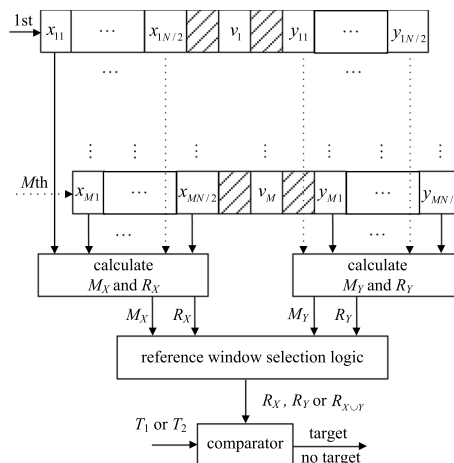


Fig. 1 The block diagram of the MRS nonparametric detector

$$\begin{cases} K_{MR}^{-1} \leq MR \leq K_{MR} \Rightarrow \text{same means} \\ MR < K_{MR}^{-1} \text{ or } MR > K_{MR} \Rightarrow \text{different means} \end{cases} \quad (2)$$

If the MR is decided to be the same, this case corresponds to homogeneous background. If the MR is made to be different, this means that the background is nonhomogeneous.

Step 2 The selection of reference window.

The MRS nonparametric CFAR will select the corresponding samples set to form the rank test statistic according to the outcomes of the MR hypothesis test. If the MR is decided to be the same, in order to enhance the detection performance of the MRS nonparametric CFAR in homogeneous background, the whole sample set $X \cup Y$ will be chosen to form the rank test statistic, it is

$$R_{X \cup Y} = \sum_{i=1}^M \sum_{j=1}^{N/2} [u(v_i - x_{ij}) + u(v_i - y_{ij})] \quad (3)$$

where $u(t)$ is the unit step function. If $R_{X \cup Y}$ exceeds the detection threshold T_1 , a target is declared to be present in the test cell. Otherwise, the target is absent.

If the MR is decided to be different, the MRS nonparametric CFAR will choose the leading reference window or the lagging one whose sample mean is larger to form the rank test statistic. This corresponds to the GO-CFAR processing. We have

$$R_X = \sum_{i=1}^M \sum_{j=1}^{N/2} u(v_i - x_{ij}) \text{ or } R_Y = \sum_{i=1}^M \sum_{j=1}^{N/2} u(v_i - y_{ij}) \quad (4)$$

If R_X or R_Y is greater than the detection threshold T_2 , the presence of a target in the test cell is declared. Otherwise, the absence of target is made.

3 The mathematical model of the MRS nonparametric CFAR

3.1 The false alarm rate of the MRS nonparametric CFAR

The MRS nonparametric CFAR selects either of the whole samples in the reference window $X \cup Y$, the samples in the leading window X or the samples in the lagging window Y for the target detection. Under the null hypothesis H_0 (the test cell contains only noise/clutter) and in homogeneous background, the test sample v_i ($i = 1, 2, \dots, M$) and the reference samples in the leading and lagging window x_{ij} and y_{ij} ($i = 1, 2, \dots, M, j = 1, 2, \dots, N/2$) are independent and identically distributed (IID) with a same distribution. When the MRS nonparametric CFAR chooses the whole samples in the reference window, the rank test statistic takes the form of

$$R_{X \cup Y} = \sum_{i=1}^M r_i = \sum_{i=1}^M \sum_{j=1}^{N/2} [u(v_i - x_{ij}) + u(v_i - y_{ij})] \quad (5)$$

where r_i is the rank of the test sample v_i on the i th pulse compared to the reference samples. It is expressed as

$$r_i = \sum_{j=1}^{N/2} [u(v_i - x_{ij}) + u(v_i - y_{ij})], \quad 0 \leq r_i \leq N \tag{6}$$

where r_i is uniformly distributed on $[0, 1, \dots, N]$ [11], that is

$$P_{r_i}^0(k) = \begin{cases} \frac{1}{N+1} & k = 0, 1, \dots, N \\ 0 & \text{other} \end{cases} \quad (i = 1, 2, \dots, M) \tag{7}$$

where $P_{r_i}^0(k)$ is the probability density function (PDF) of the rank r_i under the hypothesis H_0 .

Considering that the PDF of the sum of statistically independent variables is the convolution of their individual PDFs, the PDF of the rank test statistic $R_{X \cup Y} = \sum_{i=1}^M r_i$ for the MRS nonparametric CFAR is given by

$$P_{X \cup Y}^0(k) = P_{r_1}^0(k) * P_{r_2}^0(k) * \dots * P_{r_M}^0(k) \tag{8}$$

where “*” stands for the convolution. According to the convolution theorem, the application of the Z transform to (8) yields

$$Z\{P_{X \cup Y}^0(k)\} = Z\{P_{r_1}^0(k)\} \cdot Z\{P_{r_2}^0(k)\} \cdot \dots \cdot Z\{P_{r_M}^0(k)\} = \prod_{i=1}^M Z\{P_{r_i}^0(k)\} \tag{9}$$

where $Z\{\}$ represents the Z transform. Then

$$Z\{P_{r_i}^0(k)\} = \sum_{k=0}^{\infty} P_{r_i}^0(k) \cdot z^{-k} = \sum_{k=0}^N \frac{1}{N+1} \cdot z^{-k} = \frac{1}{N+1} \frac{1 - z^{-N-1}}{1 - z^{-1}}. \tag{10}$$

The region of convergence is $0 < |z| \leq \infty$.

Therefore, the PDF of the rank test statistic $R_{X \cup Y}$ is expressed as

$$P_{X \cup Y}^0(k) = Z^{-1}\left\{\prod_{i=1}^M Z\{P_{r_i}^0(k)\}\right\} = Z^{-1}\left\{\frac{1}{(N+1)^M} \frac{(1 - z^{-N-1})^M}{(1 - z^{-1})^M}\right\} \tag{11}$$

where $Z^{-1}\{\}$ denotes the inverse Z transform.

Under the hypothesis H_0 , if the MRS nonparametric CFAR selects the whole samples in the reference window for target detection, the false alarm rate of the MRS nonparametric CFAR takes the form of

$$P_{fa}^{X \cup Y} = \sum_{k=T_1}^{\infty} P_{X \cup Y}^0(k) \tag{12}$$

For a given false alarm rate, the detection threshold T_1 of the MRS nonparametric CFAR can be solved by (12). If $R_{X \cup Y}$ is greater than the detection threshold T_1 , a target is declared to be present. Otherwise, no target exists.

If the MRS nonparametric CFAR chooses the samples in the leading or lagging window X or Y for target detection, the PDF $P_X^0(k)$ or $P_Y^0(k)$ of the rank test statistic R_X

or R_Y can also be obtained by (11), except that N is replaced by $N/2$. Accordingly, the false alarm rate of the MRS nonparametric CFAR when the leading or lagging window is selected for target detection can be given by $P_{fa}^X = \sum_{k=T_2}^{\infty} P_X^0(k)$ or $P_{fa}^Y = \sum_{k=T_2}^{\infty} P_Y^0(k)$, respectively. It is noted that the detection threshold T_2 is used here.

Since the MRS nonparametric CFAR selects either of the sample set $X \cup Y$, X or Y to make the target decision, the whole false alarm probability of the MRS nonparametric CFAR can be expressed as

$$P_{fa} = P(X \cup Y)P_{fa}^{X \cup Y} + P(X)P_{fa}^X + P(Y)P_{fa}^Y \tag{13}$$

where $P(X \cup Y)$, $P(X)$ and $P(Y)$ is the probability of the MRS nonparametric CFAR to choose the sample set $X \cup Y$, X or Y , respectively. When the design false alarm rate is required at $P_{fa} = \alpha$, setting $P_{fa}^{X \cup Y} = P_{fa}^X = P_{fa}^Y = \alpha$, then $P_{fa} = [P(X \cup Y) + P(X) + P(Y)]\alpha = \alpha$. Since $P(X \cup Y) + P(X) + P(Y) = 1$, the whole false alarm probability of the MRS nonparametric CFAR is still $P_{fa} = \alpha$. Therefore, the MRS nonparametric CFAR can maintain a constant false alarm rate in a homogeneous background, which is irrelevant to the distribution of background clutter.

3.2 The detection probability of the MRS nonparametric CFAR

In order to analyze the detection performance of the MRS nonparametric CFAR, Gaussian distributed background and Swerling II target fluctuation model are considered here. In a homogeneous background, it is assumed that the square-law detected outputs for any range cells in each pulse are independent and identically distributed. Under the alternative hypothesis H_1 (the presence of a target in the test cell), the PDF and cumulative distribution function (CDF) of the sample in the test cell containing target signal is given by, respectively

$$g(t) = \frac{1}{\mu(1 + \lambda)} \exp \left[-\frac{t}{\mu(1 + \lambda)} \right] u(t) \tag{14}$$

and

$$G(t) = 1 - \exp \left[-\frac{t}{\mu(1 + \lambda)} \right] u(t) \tag{15}$$

where μ is the total clutter-plus-thermal noise power, λ is the average signal-to-noise power ratio (SNR) of the target. In a homogeneous background, letting $\lambda = 0$, the PDF and CDF of the noise sample $f(t)$ and $F(t)$ can be obtained from (14) and (15), respectively.

Under the hypothesis H_1 , when the MRS nonparametric CFAR selects the whole samples in the reference window for target detection, the probability of the rank of the test sample $r_i = k$ is obtained by

$$\begin{aligned}
 P_{r_i}^1(k) &= \int_0^\infty \binom{N}{k} [F(t)]^k [1 - F(t)]^{N-k} g(t) dt \\
 &= \frac{1}{\mu(1 + \lambda)} \int_0^\infty \binom{N}{k} \left[1 - \exp\left(-\frac{t}{\mu}\right) \right]^k \\
 &\quad \times \left[\exp\left(-\frac{t}{\mu}\right) \right]^{N-k} \exp\left(-\frac{t}{\mu(1 + \lambda)}\right) dt \\
 &= \frac{1}{1 + \lambda} \binom{N}{k} \frac{\Gamma[N - k + 1/(1 + \lambda)] \Gamma(k + 1)}{\Gamma[N + 1 + 1/(1 + \lambda)]}
 \end{aligned} \tag{16}$$

Under the hypothesis H_1 , by means of the convolution theorem, the PDF of the rank test statistic $R_{X \cup Y} = \sum_{i=1}^M r_i$ when the MRS nonparametric CFAR selects the whole samples in the reference window is given by

$$P_{X \cup Y}^1(k) = Z^{-1} \left\{ \left[Z \left\{ P_{r_i}^1(k) \right\} \right]^M \right\} \tag{17}$$

Therefore, under the hypothesis H_1 , when the MRS nonparametric CFAR selects the whole samples in the reference window for target detection, the detection probability of the MRS nonparametric CFAR is obtained as

$$P_d^{X \cup Y} = \sum_{k=T_1}^\infty P_{X \cup Y}^1(k) \tag{18}$$

Under the hypothesis H_1 , if the MRS nonparametric CFAR chooses the samples in the leading or lagging window X or Y for target detection, the PDF $P_X^1(k)$ or $P_Y^1(k)$ of the rank test statistic R_X or R_Y can also be obtained by (17), except that N is replaced by $N/2$. Similarly, the detection probability of the MRS nonparametric CFAR with the choice of the leading or lagging window can be given by $P_d^X = \sum_{k=T_2}^\infty P_X^1(k)$ or $P_d^Y = \sum_{k=T_2}^\infty P_Y^1(k)$, respectively.

Since the MRS nonparametric CFAR selects either of the sample set $X \cup Y$, X or Y for target detection, the whole detection probability of the MRS nonparametric CFAR is formulated as

$$P_d = P(X \cup Y) P_d^{X \cup Y} + P(X) P_d^X + P(Y) P_d^Y \tag{19}$$

3.3 The false alarm rate of the MRS nonparametric CFAR at clutter edge

The clutter edge occurs when the total noise/clutter power received within the reference window changes abruptly. The clutter edge is modeled as a step function discontinuity in the background power here. We assume that there are L cells coming from heavy clutter region, whereas $N-L$ cells from weak noise. The CDF of the weak noise sample is shown as

$$F(t) = \left[1 - \exp\left(-\frac{t}{\mu}\right) \right] u(t) \tag{20}$$

and the CDF of the strong clutter sample has a form of

$$\bar{F}(t) = \left[1 - \exp\left(-\frac{t}{\gamma\rho}\right) \right] u(t) \tag{21}$$

where γ denotes the power ratio between the heavy clutter and the weak noise. When the MRS nonparametric CFAR selects the whole samples $X \cup Y$ in the reference window for target detection, the expression of the false alarm rate at clutter edges in this situation is given by [11]

$$\bar{P}_{fa}^{X \cup Y} = \sum_{k=T_1}^{\infty} Z^{-1} \left\{ [Z\{\bar{P}_{r_i}(k)\}]^M \right\} \tag{22}$$

where

$$\begin{aligned} \bar{P}_{r_i}(k) = & \sum_{j=\max(0, k-L)}^{\min(k, N-L)} \binom{N-L}{j} \binom{L}{k-j} \sum_{i_1=0}^j \binom{j}{i_1} (-1)^{i_1} \\ & \times \frac{\Gamma[\gamma(i_1 + N - L - j) + L - k + j + 1] \Gamma[k - j + 1]}{\Gamma[\gamma(i_1 + N - L - j) + L + 2]} \quad (k = 0, 1, \dots, N) \end{aligned} \tag{23}$$

In a clutter boundary environment, if the MRS nonparametric CFAR selects the samples in the leading or lagging window X or Y for target detection, the corresponding false alarm rate \bar{P}_{fa}^X and \bar{P}_{fa}^Y can also be obtained by (22), except that N is replaced by $N/2$ and T_1 by T_2 .

Considering that the MRS nonparametric CFAR selects either of the sample set $X \cup Y$, X or Y for target detection, the whole false alarm rate of the MRS nonparametric CFAR at clutter edge is formulated as

$$P_{fa} = P(X \cup Y) \bar{P}_{fa}^{X \cup Y} + P(X) \bar{P}_{fa}^X + P(Y) \bar{P}_{fa}^Y \tag{24}$$

4 Performance analysis and numerical result

Here, we make use of the analytical expressions derived in the previous section and the importance sampling technique to evaluate the performance of the MRS nonparametric CFAR in homogeneous background, multiple targets situation and clutter edges, and make a comparison to that of the classical RS nonparametric CFAR along with some conventional parametric CFAR detectors.

4.1 Performance analysis in homogeneous background and in multiple targets situation

In order to fairly analyze the performance of the CFAR detectors considered here, the same nominal false alarm rate $P_{fa} = 10^{-6}$, the length of the whole reference window $N=36$, and the number of the multiple pulses $M=8$ are selected for them. A special parameter of the MRS nonparametric CFAR is the threshold parameter K_{MR} . As K_{MR} increases, the error probability such that the means in the leading and lagging windows in homogeneous environment is decided as different decreases, and the sensitivity to distinguish them at clutter edges also decreases. On the other hand, as K_{MR} decreases, the leading or lagging reference window will be used more frequently in homogeneous background and in multiple targets situation, thus, the additional CFAR loss will

increase. Therefore, there is a compromise for the selection of K_{MR} . As suggested in [6], the error probability of the means in the leading and lagging windows in homogeneous environment being decided as different takes 0.1, this corresponds to a parameter value of $K_{MR} = 1.35$ in our situation. For the nominal false alarm rate $P_{fa} = 10^{-6}$, the detection threshold of the MRS nonparametric CFAR takes $T_1 = 267$ or $T_2 = 135$ which can be calculated by (11) and (12).

In the case of $M = 8$, $N = 36$ and $K_{MR} = 1.35$, Fig. 2 gives the probability of selecting the sample set X in the leading window, the sample set Y in the lagging window and the whole sample set $X \cup Y$ for the MRS nonparametric CFAR in homogeneous background. In the figure, the probability of selecting the sample set X in the leading window, the sample set Y in the lagging window and the whole sample set $X \cup Y$ is denoted by $P(X)$, $P(Y)$ and $P(X \cup Y)$, respectively. It can be seen that the MRS nonparametric CFAR selects the whole sample set $X \cup Y$ at nearly probability 1, and it selects the sample set X or Y at approximate probability 0 in homogeneous background.

We assume a Swerling II fluctuation model for interfering target and it has the same SNR as the primary target. When the number of interfering target in the leading window is $IL = 1$ and that in the lagging window is $IR = 0$ (This interfering targets situation is denoted by $(IL = 1, IR = 0)$, the same in the following), Fig. 3 illustrate the probability for the MRS detector selecting the sample set X , Y or $X \cup Y$ versus SNR in this case. It can be observed that if SNR is small, the MRS nonparametric CFAR most probably selects the whole sample set $X \cup Y$ for target detection, if SNR gets large, the MRS nonparametric CFAR most likely selects the sample set X in the leading window for target detection as expected.

In homogeneous background and in multiple targets situation ($IL = 1, IR = 0$), for $M = 8$, $N = 36$ and $K_{MR} = 1.35$, Fig. 4 gives the detection probability of the MRS nonparametric CFAR versus SNR (dB), with a comparison to that of the classical RS nonparametric CFAR. In the figure, notation “MRS(1,0)” denotes the detection

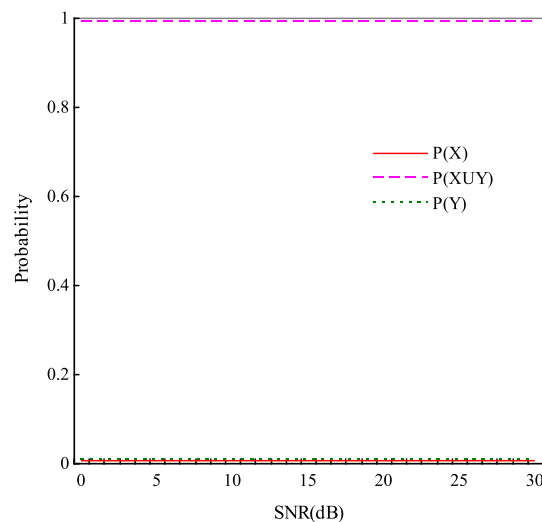


Fig. 2 The probability for the MRS detector selecting the sample set X , Y or $X \cup Y$ versus SNR in homogeneous background

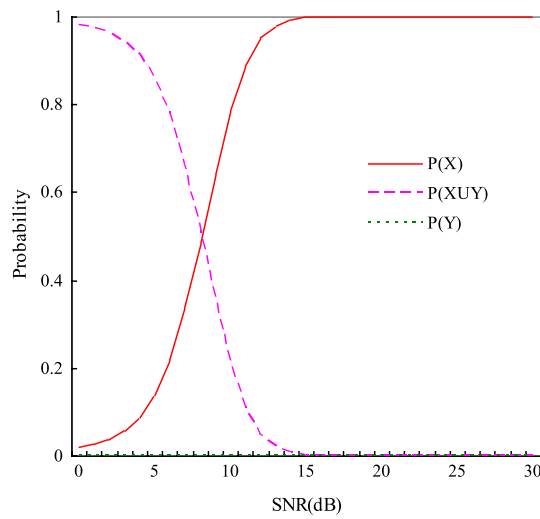


Fig. 3 Probability for the MRS detector selecting the sample set X , Y or $X \cup Y$ versus SNR ($IL = 1$, $IR = 0$)

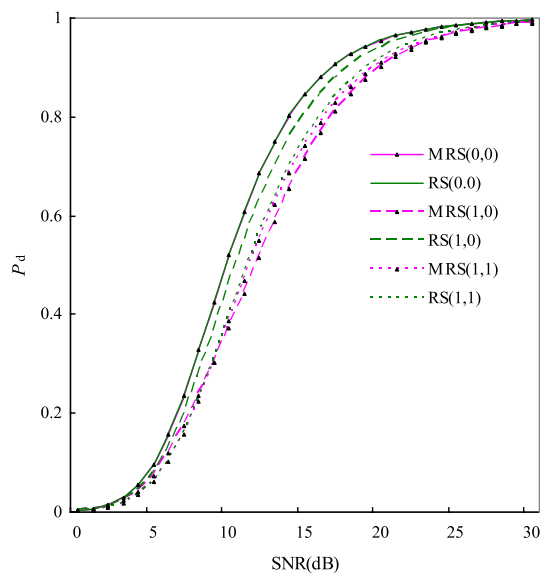


Fig. 4 The detection probability of the MRS detector versus SNR in homogeneous background

probability of the MRS nonparametric CFAR with $IL = 1$ and $IR = 0$. It can be seen that the curve of the MRS nonparametric CFAR and that of the RS nonparametric CFAR almost overlap together in homogeneous background. In multiple target situations ($IL = 1$, $IR = 0$) and ($IL = 1$, $IR = 1$), the detection performance of the MRS nonparametric CFAR approximates to that of the classical RS nonparametric CFAR.

If more interfering targets enter the leading window or the lagging window, for $M = 8$, $N = 36$ and $K_{MR} = 1.35$, Fig. 5 shows the detection probability of the MRS nonparametric CFAR versus SNR (dB), compared with that of the classical RS nonparametric CFAR. The maximum number of the interfering targets such that a reference window can accommodate can be estimated by $\text{INT}\{(MN - T)/M\}$, where $\text{INT}\{x\}$

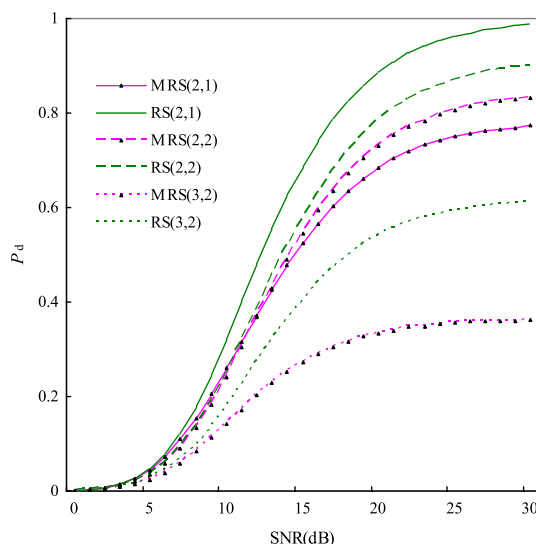


Fig. 5 The detection probability of the MRS detector versus SNR in multiple targets situation

rounds x to the nearest integer, and the N is the sample number in the reference window. For the leading or lagging window, the allowable number of interfering targets is 1, and that is 3 for the whole reference window here. In Fig. 4, the number of interfering targets in the leading window or lagging windows is not exceed 1, therefore, the detection performance of the MRS nonparametric CFAR approaches that of the RS nonparametric CFAR. In Fig. 5, the number of interfering targets is more than the allowable number for the MRS nonparametric CFAR, thus the detection performance of the MRS nonparametric CFAR greatly degrades relative to that of the RS nonparametric CFAR. If the allowable number of interfering targets exceeds that of the MRS and RS nonparametric CFAR detectors, i.e., (2, 2) or (3, 2), the detection performance for the MRS and RS nonparametric CFAR detectors substantially deteriorates.

4.2 Performance analysis at clutter edge

Here, we analyze the false alarm performance of the MRS nonparametric CFAR at clutter edge. We model a clutter boundary as a step function discontinuity in clutter power. Figure 6 gives the probability for the MRS detector selecting the sample set X , Y or $X \cup Y$ versus the number L of the reference cells immersed in heavy clutter, for $M=8$, $N=36$, $\gamma=10$ dB and $K_{MR}=1.35$. It can be seen that when the clutter boundary moves into the reference window, the MRS nonparametric CFAR gradually selects the leading window for target detection, and when a large proportion of the reference window enter the heavy clutter, the MRS nonparametric CFAR eventually selects the whole reference window for target detection with a high possibility. Figure 7 shows the false alarm probability P_{fa} of the MRS nonparametric CFAR as a function of the number L of the reference cells immersed in heavy clutter for $M=8$, $N=36$ and $\gamma=5$ dB, 10 dB, 15 dB. In the figure, the false alarm probability P_{fa} of the classical RS nonparametric CFAR is added for a comparison. It can be seen that if $L \leq N/2$, the

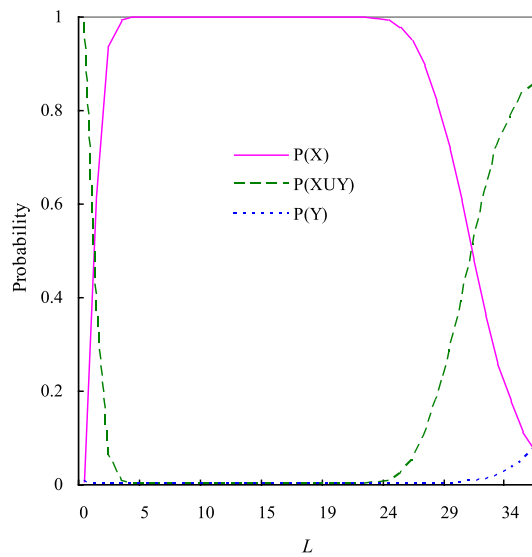


Fig. 6 The probability for the MRS detector selecting X , Y or $X \cup Y$ versus the number L of cells entering the strong clutter region ($\gamma = 10$ dB)

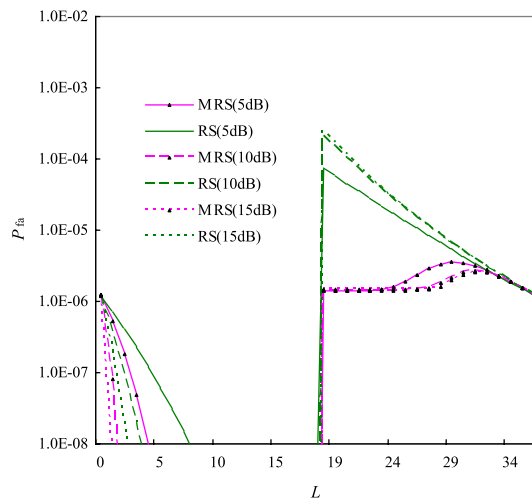


Fig. 7 The false alarm probability for the MRS detector versus the number L of cells entering the strong clutter region

P_{fa} of the classical RS nonparametric CFAR decreases, whereas if $L > N/2$, that of the classical RS nonparametric CFAR exhibits a sharp increase. The latter case seriously degrades the performance of a detector since it violates the CFAR constraint. However, in the case of $L > N/2$, the rise of the false alarm rate for the MRS nonparametric CFAR is more gently than that of the classical RS nonparametric CFAR, and the highest value of the false alarm rate for the MRS nonparametric CFAR is within an order of magnitude for the nominal false alarm rate. From the numerical results, it can be seen that the ability of the MRS nonparametric CFAR to control the rise of false alarm rate at clutter edges is evidently improved relative to that of the classical RS nonparametric CFAR.

4.3 The comparison with several conventional parametric CFAR detectors

In order to have a relatively complete analysis of the performance for the MRS nonparametric CFAR, a comparison of the detection performance and false alarm rate in homogeneous background and nonhomogeneous situation caused by interfering targets and clutter edges with that several conventional parametric CFAR, i.e., the CA-CFAR, the GO-CFAR and the OS-CFAR with M pulses integration, is made in this section. The same $M=8$, $N=36$, the nominal false alarm rate $P_{fa} = 10^{-6}$ and the Gaussian distributed background are considered for these CFAR schemes. For the MRS nonparametric CFAR, the $K_{MR}=1.35$ is taken as before. For the OS-CFAR with incoherent integration, the representative ordered sample $k=32$ is used to set an adaptive detection threshold. Figure 8 shows the detection performance of the MRS nonparametric detector as a function of SNR in homogenous background. As a comparison, the P_d the CA-CFAR, the GO-CFAR and the OS-CFAR with M pulses integration are also added. It can be seen that the P_d curves of the CA-CFAR, the GO-CFAR and the OS-CFAR with incoherent integration almost overlap together, and the detection performance of the MRS detector exhibits an evident loss in SNR. It is noticed that an additional loss of nearly 5 dB is required for the MRS nonparametric detector to reach $P_d=0.5$ relative to the parametric CFAR detectors. This is the price for the MRS nonparametric CFAR to have a virtue that its false alarm rate is irrelative to the distribution type of background clutter.

In multiple targets situation (1, 1), i.e., the number of interfering targets in both the leading and lagging window is 1. Figure 9 illustrates the detection performance of the MRS nonparametric detector as a function of SNR. In order to evaluate the ability of the MRS nonparametric detector to accommodate the interfering targets, the interfering target to noise power ratio (INR) is assumed as $INR=30$ dB here. It is observed that the CA-CFAR and the GO-CFAR with incoherent integration almost lose their detection abilities in the strong interfering targets situation. It can be seen that the P_d of the CA-CFAR or the GO-CFAR with incoherent integration is nearly equal to 0 at $SNR=20$ dB,

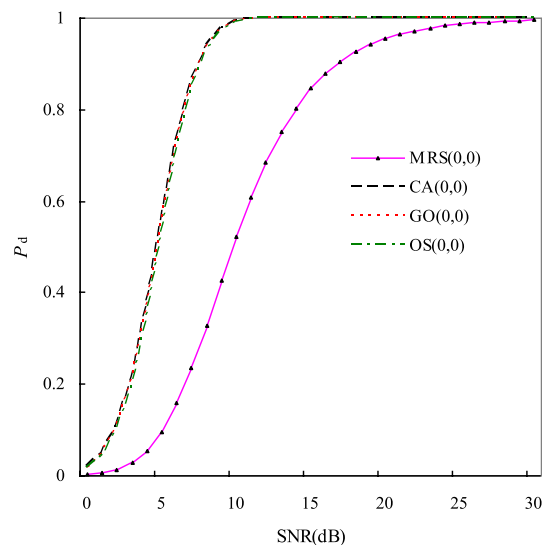


Fig. 8 The comparison of P_d of the MRS detector with several parametric CFAR detectors in homogeneous background

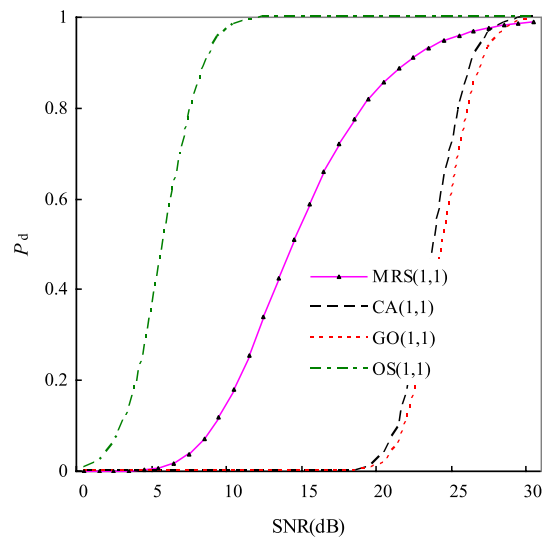


Fig. 9 The comparison of P_d of the MRS detector with several parametric CFAR detectors in multiple targets situation, INR = 30 dB

whereas the P_d of the MRS nonparametric detector gives a value of $P_d = 0.86$ in this case. The best detection performance in multiple targets situation is obtained by the OS-CFAR with incoherent integration as expected.

Although the classical RS nonparametric detector has the advantage that its false alarm rate is irrelative to the distribution type of background clutter, its false alarm rate still shows a sharp rise at clutter edges. In order to improve its false alarm performance at clutter edges, the MRS nonparametric detector is proposed by introduction of VI-CFAR idea to the classical RS nonparametric detector. Here, we consider a possible practical situation of clutter edge that the Weibull clutter with a shape parameter $c = 1.2$ shifts into a noise dominating background ($c = 2.0$). The nominal false alarm rate of these detectors is originally set at $P_{fa} = 10^{-6}$ according to a Gaussian background with $c = 2.0$. Figure 10 makes a comparison of the false alarm performance for the MRS detector to that of the CA-CFAR, GO-CFAR and OS-CFAR with incoherent integration, as a function of the number L of the reference cells immersed in clutter. The clutter to noise power ratio is $\gamma = 10$ dB. It can be seen that when the heavy clutter with $c = 1.2$ moves into the reference window, the false alarm rate of the CA-CFAR, GO-CFAR and OS-CFAR with incoherent integration increases more than three orders of magnitude and can not return to the nominal false alarm rate $P_{fa} = 10^{-6}$. However, the rise of the false alarm rate for the MRS nonparametric detector changes smoothly and is within 1 order of magnitude for the nominal false alarm rate, and also return to the original design value.

5 Conclusion

The classical RS nonparametric CFAR plays an important role in the practical applications of radar target detection. In order to improve the false alarm performance of the RS nonparametric CFAR at clutter edges, a modified rank sum (MRS) nonparametric CFAR based on the mean ratio of the samples in the leading and lagging windows is

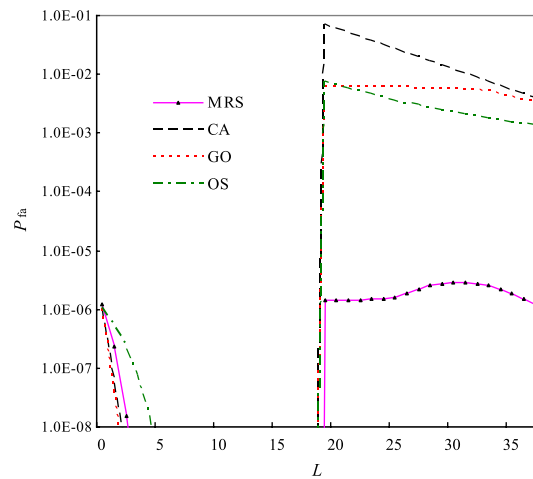


Fig. 10 The comparison of P_{fa} of the MRS detector with several parametric CFAR detectors at clutter edges, $\gamma = 10$ dB

proposed. The analytical expressions of the detection probability and false alarm rate of the MRS nonparametric CFAR in homogeneous background along with that of the false alarm rate at clutter edges are derived, and a comparison to the performance of the classical RS nonparametric CFAR as well as that of the CA-CFAR, GO-CFAR and OS-CFAR with incoherent integration in homogeneous background, multiple targets situation and clutter edges is made. It is shown that the detection performance of the MRS nonparametric CFAR in homogeneous background and a moderate number of interfering targets situation is close to that of the classical RS nonparametric detector, and its ability to control the rise of the false alarm rate at clutter edges is evidently improved. Since the classical RS nonparametric CFAR has the virtue of the simplicity of hardware implementation, and the only additional operation of the MRS nonparametric CFAR relative to the classical RS nonparametric CFAR is the MR hypothesis decision, thus the MRS nonparametric CFAR is also easy to be implemented. The parameters K_{MR} , K_{MR}^{-1} , T_1 and T_2 can be determined in advance and stored in a look-up table in a practical system with programmable signal processing. There are 2 cases for the computational complexity of the MRS nonparametric CFAR, if the MRS nonparametric CFAR selects the whole samples in the reference window for the target detection, the computational complexity of the MRS nonparametric CFAR needs $M \cdot N - 2$ addition operations, 1 division operation, $M \cdot N + 3$ comparisons and 1 accumulator; if the MRS nonparametric CFAR takes the samples in the leading or lagging window for target detection, it needs $M \cdot N - 2$ addition operations, 1 division operation, $M \cdot N/2 + 3$ comparisons and 1 accumulator.

It should be noted, the variability index generalized sign (VI-GS) which combines the VI-CFAR and the RS nonparametric CFAR is proposed in [12]. Also, the variability index modified rank squared (VI-MRS) nonparametric detector is proposed in [13], which combines the VI-CFAR with the modified rank squared (MRS) nonparametric detector. However, both of them lack the analytical expressions for the detection probability and the false alarm rate for the VI-GS or VI-MRS in homogeneous background and nonhomogeneous environment caused by multiple targets and clutter edge, and lack the performance analysis of the VI-GS or VI-MRS in clutter boundaries. It is noted that

the idea to enhance the performance of the classical RS and RQ nonparametric detectors in nonhomogeneous background caused by multiple targets and clutter edge by means of the sub-window technique was first given in [14], and a detail description of detection scheme for the MRS nonparametric CFAR and the modified rank quantization (MRQ) CFAR by means of the VI-CFAR and the ODV technique [15] has been presented in the application form of “The theory and application of nonparametric CFAR detection” (The National Natural Science Foundation of China, No. 61179016) in Mar. 2011.

Abbreviations

CFAR	Constant false alarm rate
CA	The cell-averaging
GO	The greatest-of
SO	The smallest-of
OS	The order-statistic
RS	The rank sum
RQ	The rank quantization
SNR	The average signal-to-noise power ratio
MRS	The modified RS nonparametric
PDF	Probability density function
CDF	Cumulative distribution function

Acknowledgements

We thank the reviewers for many helpful comments and suggestions, which have considerably enhanced this work.

Funding

This work is supported by the National Natural Science Foundation of China under Grant Nos. 62171402 and 61179016.

Availability of data and materials

Data sharing is not applicable to this article.

Declarations

Ethics approval and consent to participate

Not applicable.

Consent for publication

Approved.

Competing interests

The authors declare that they have no competing interests.

Received: 20 December 2022 Accepted: 8 June 2023

Published online: 27 June 2023

References

1. J. Karvonen, A. Gegiuc, T. Niskanen, A. Montonen, J. Buus-Hinkler, E. Rinne, Iceberg detection in dual-polarized C-band SAR imagery by segmentation and nonparametric CFAR (SnP-CFAR). *IEEE Trans. Geosci. Remote Sens.* (2022). <https://doi.org/10.1109/TGRS.2021.3070312>
2. T. Jeong, S. Park, J.W. Kim, J.W. Yu, Robust CFAR detector with ordered statistic of sub-reference cells in multiple target situations. *IEEE Access* **10**, 42750–42761 (2022). <https://doi.org/10.1109/ACCESS.2022.3168707>
3. R.G. Zefreh, M.R. Taban, M.M. Naghsh, S. Gazor, Robust CFAR detector based on censored harmonic averaging in heterogeneous clutter. *IEEE Trans. Aerosp. Electron. Syst.* **57**(3), 1956–1963 (2021). <https://doi.org/10.1109/TAES.2020.3046050>
4. F.D.A. Garcia, H.R.C. Mora, G. Fraidenaich, J.C.S.S. Filho, Square-law detection of exponential targets in Weibull distributed ground clutter. *IEEE Geosci. Remote Sens. Lett.* **18**(11), 1956–1960 (2021). <https://doi.org/10.1109/LGRS.2020.3009304>
5. M.B. El Mashade, Heterogeneous performance assessment of new approach for partially-correlated χ^2 -targets adaptive detection. *Radioelectron. Commun. Syst.* **64**(12), 633–648 (2021). <https://doi.org/10.3103/S0735272721120025>
6. M.E. Smith, P.K. Varshney, Intelligent CFAR processor based on data variability. *IEEE Trans. Aerosp. Electron. Syst.* **36**(3), 837–847 (2000). <https://doi.org/10.1109/7.869503>
7. G.M. Dillard, R.A. Dillard, Radar automatic detection. *Microw. J.* **28**(6), 125–130 (1985)
8. V.G. Hansen, B.A. Olsen, Nonparametric radar extraction using a generalized sign test. *IEEE Trans. Aerosp. Electron. Syst.* **7**(5), 942–950 (1971). <https://doi.org/10.1109/TAES.1971.310335>

9. G.W. Zeoli, T.S. Fong, Performance of a two-sample Mann-Whitney nonparametric detector in a radar application. *IEEE Trans. Aerosp. Electron. Syst.* **7**(5), 951–959 (1971). <https://doi.org/10.1109/TAES.1971.310336>
10. M. Sekine, Y.H. Mao, *Weibull Radar Clutter* (Peter Peregrinus Ltd., London, 1990)
11. X.W. Meng, Rank sum nonparametric CFAR detector in nonhomogeneous background. *IEEE Trans. Aerosp. Electron. Syst.* **57**(1), 397–403 (2021). <https://doi.org/10.1109/TAES.2020.3017319>
12. L. Zhang, Z.J. Zhao, J. Guan, Y. He, An intelligent nonparametric GS detection algorithm based on adaptive threshold selection. *J. Radars* **1**(4), 387–392 (2012). <https://doi.org/10.3724/SPJ.1300.2012.20084>. (In Chinese)
13. X. D. Li, B. N. Pei, Y.H. Zhang, An improved nonparametric detector for nonhomogeneous clutter environment, in *2014 Symposium on Computer Applications and Communications* (Weihai, 2014), pp. 10–13
14. X.W. Meng, Research on CFAR Detection Schemes for Radar Target, Ph.D. dissertation (Naval Aeronautical and Astronautical University, 2008)
15. A. Farrouki, M. Barkat, Automatic censoring CFAR detector based on ordered data variability for nonhomogeneous environments. *IEE Proc. Radar Sonar Navig.* **152**(1), 43–51 (2005). <https://doi.org/10.1049/ip-rsn:20045006>

Publisher's Note

Springer Nature remains neutral with regard to jurisdictional claims in published maps and institutional affiliations.

Submit your manuscript to a SpringerOpen[®] journal and benefit from:

- ▶ Convenient online submission
- ▶ Rigorous peer review
- ▶ Open access: articles freely available online
- ▶ High visibility within the field
- ▶ Retaining the copyright to your article

Submit your next manuscript at ▶ [springeropen.com](https://www.springeropen.com)
